Voluntary Energy Harvesting Relays and Selection in Cooperative Wireless Networks

Bhargav Medepally and Neelesh B. Mehta, *Senior Member, IEEE*

***Abstract*—The use of energy harvesting (EH) nodes as cooperative relays is a promising and emerging solution in wireless systems such as wireless sensor networks. It harnesses the spatial diversity of a multi-relay network and addresses the vexing problem of a relay's batteries getting drained in forwarding information to the destination. We consider a cooperative system in which EH nodes volunteer to serve as amplify-and-forward relays whenever they have sufficient energy for transmission. For a general class of stationary and ergodic EH processes, we introduce the notion of energy constrained and energy unconstrained relays and analytically characterize the symbol error rate of the system. Further insight is gained by an asymptotic analysis that considers the cases where the signal-to-noise-ratio or the number of relays is large. Our analysis quantifies how the energy usage at an EH relay and, consequently, its availability for relaying, depends not only on the relay's energy harvesting process, but also on its transmit power setting and the other relays in the system. The optimal static transmit power setting at the EH relays is also determined. Altogether, our results demonstrate how a system that uses EH relays differs in significant ways from one that uses conventional cooperative relays.**

***Index Terms*—Energy harvesting, relays, selection, cooperative systems, diversity methods, modulation, fading channels, amplify-and-forward, energy storage, wireless sensor networks.**

I. Introduction

COOPERATIVE communication using relays promises significant improvements in throughput and reliability. Several cooperation schemes make use of one or more relays to forward to the destination a representation of the signal they have received from the source [1]–[6]. When multiple nodes are present, several cooperation schemes select the relay with the best instantaneous channel state [3], [7], [8], where the specifics of the cooperation protocol determine what 'best' means. Such single relay selection is of practical interest because it harnesses spatial diversity and, yet, avoids the tight synchronization otherwise required among multiple geographically separated relays.

In forwarding to the destination a representation of the signal it has received from the source, a relay expends its own energy. Since running power cables to supply energy is often impractical or cumbersome in several scenarios, this energy is typically supplied by a pre-charged battery. Unfortunately, the more often a relay is selected, the sooner its battery drains out. Once the battery drains out, the relay can no longer assist in transmission. While fairness mechanisms [9] or network lifetime maximization approaches [10] can be used to balance the energy drain across multiple relays, they only delay the inevitable – all the relays still do eventually run out of energy.

An alternate emerging solution is the use of energy harvesting (EH) nodes as relays. These nodes harvest energy from the environment to carry out their communication tasks [11]–[13]. Energy is harvested using solar, vibration, thermoelectric effects, and other physical phenomena [14], [15]. An EH node that drains out its battery can harvest energy later and again become available for relaying. Thus, EH nodes are attractive as they promise perpetual network lifetime without the need for periodic battery replacements or external power cables. Consequently, they hold great promise in applications such as wireless sensor networks.

A key aspect that affects an EH node's performance is its *energy profile*, which mathematically models the energy harvested at the EH node as a function of time. In general, the energy profile depends on the device physics [11], [16], [17]. Various analytical models for it have been considered. For example, a leaky bucket model, motivated by Internet traffic modeling, was used in [11]. Alternately, a stochastic Markov model was used in [18]. A simpler, but analytically tractable, Bernoulli probabilistic energy injection model was used in [16], [17].

Depending on the energy profile, the harvested energy is often available in random and small amounts and only sporadically. Storing the excess harvested energy in a battery or a super-capacitor for later use helps mitigate this randomness, but only partially. Fundamentally, it is the *energy harvesting profile* that determines how effective an EH relay can be in a cooperative system. *In general, the energy neutrality constraint, which mandates that the energy used by the relay cannot exceed the energy harvested by it, imposes fundamental limitations on the end-to-end system performance and forces the transmit power settings of the relay to be carefully optimized.* For example, increasing the transmit energy improves the reliability of transmissions by the relay. However, it also uses up an EH relay's harvested energy, thereby decreasing the odds that it will volunteer as a relay later. Fewer relays to choose from, in turn, reduces the spatial diversity that can be harnessed by the system. For example, when the kth ($k \geq 2$) best relay is chosen because the best $k-1$ relays are unavailable due to lack of energy, the diversity order decreases from $N+1$ to $N-k+2$ [19]. Thus, while energy harvesting has benefits, it comes at the cost of a more involved link and network design [16], [20].

Understanding the performance benefits of using EH relays

Manuscript received March 22, 2010; revised June 22, 2010; accepted August 1, 2010. The associate editor coordinating the review of this paper and approving it for publication was C.-F. Chiasserini.

B. Medepally is with ST-Ericsson, Bangalore, India (e-mail: bhargavmvpk@gmail.com).

N. B. Mehta is with the Electrical Communication Engineering Dept., Indian Institute of Science (IISc), Bangalore, India (e-mail: nbmehta@ece.iisc.ernet.in).

This work was partially supported by a research grant from the DRDO-IISc Program on Mathematical Engineering.

A part of this work has appeared in the IEEE Intl. Conf. Commun. (ICC), Cape Town, South Africa, May 2010.

Digital Object Identifier 10.1109/TWC.2010.091510.100447

and optimizing their usage is, thus, an important and challenging problem, and is the focus of this paper. We shall analyze a system that uses multiple EH cooperative amplify-and-forward (AF) relays. We focus on AF relaying because it has been considered to be suitable for wireless sensor networks that require low complexity nodes, and has been well investigated in the literature [3]–[5], [7]–[9], [21], [22]. In our system, the EH nodes volunteer to relay if and only if they have enough energy to transmit the data.

We develop the analysis for the general case in which the source-to-relay (SR) channels and the relay-to-destination (RD) channels are not identical, as is often the case in practical deployments of relays. To highlight the inter-relationships between the various system parameters, we also present intuitive and simpler results for the special case in which SR channels are statistically identical and so are the RD channels. Our analysis only requires that the energy harvesting process is stationary and ergodic. It, thus, applies to several energy harvesting profiles discussed in the literature [16]–[18]. Considerable further insight is gained by analyzing two asymptotic regimes: (i) when the number of EH relays is large and the total energy harvested by the system is kept fixed, and (ii) when the mean channel gains of the various links are large. The analysis also leads to a general characterization of the conditions under which the EH nodes operate in an *energy unconstrained* regime, where the randomness in energy harvesting no longer affects an EH relay's availability. As we shall see, this plays an important role in determining the optimal transmit power settings at an EH relay. The sum total of our results shows that systems that use voluntary EH relays differ in several respects from conventional cooperative systems and provide an attractive solution for improving performance.

The paper is organized as follows. Section II sets up the energy harvesting and relay cooperation model. The analysis is developed for the symmetric and general cases in Sections III and IV, respectively. Simulations are presented in Section V, and are followed by our conclusions in VI. Several mathematical details are relegated to the Appendix.

II. System Model: Energy Harvesting and Cooperation Aspects

As shown in Figure 1, the system we consider consists of a source (S), a destination (D), and N energy harvesting AF relays $1, \ldots, N$. The source and destination nodes are conventional nodes that want to communicate with each other. The various SR and RD channels, and the source-to-destination (SD) channel are assumed to be independent, as is typically the case when the source, relays, and destination are spaced several wavelengths apart in a rich scattering environment. However, *the channels need not be identically distributed.* The channel gains for the source-to-Relay-i (S–i) and Relay-i-to-destination (i–D) channels are denoted by h_{si} and h_{id}, respectively. The direct SD channel gain is denoted by h_{sd}. The inter-relay channels do not matter and are, therefore, not specified. The cooperative transmission of δ MPSK symbols, $x_1, \ldots, x_\delta$, takes place over two phases, each of duration T_p sec [1], [4], [8]. In the first phase, S transmits $x_1, \ldots, x_\delta$ with power P_s, which is received by the destination and relays. In the second phase, one of the relays amplifies and forwards the signal it has received to the destination. Note that it is possible that due to the energy harvesting nature of the relays, no relay is available in the second time slot. At the end of the second time slot, the destination optimally combines the signals it has received in the two time slots. All channels are frequency-flat, block-fading Rayleigh channels that remain constant over at least the duration of the two phases of cooperative transmission.

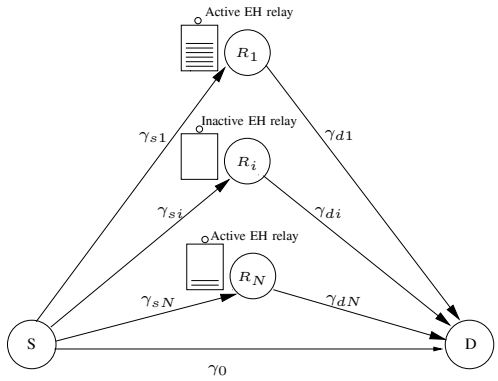

Fig. 1. Voluntary energy harvesting relays with battery storage capability that assist cooperative communication between a source and a destination.

A. Energy Harvesting and Energy Storage Model

The energy harvested by a Relay i over time is assumed to be a stationary and ergodic process, with mean E_i^{av} J/sec. No other limiting assumptions about it are made in our analysis. Thus, this general model encompasses several energy harvesting profiles assumed in the literature. For example, in [16], [17], an energy E_s is harvested with a fixed probability every T_p seconds. The model also encompasses multiple- or continuous-valued harvested energy and time correlations, if any. A simple example of this is the Markov model-based profile used in [18].

The EH relay stores its harvested energy in its battery or a super-capacitor [13], and draws energy from it to transmit. The battery or super-capacitor helps the EH relay partially overcome the randomness in the energy harvested. To ensure analytical tractability, the energy storage capacity is assumed to be large. Also, the leakage within the battery or super-capacitor and the inefficiency in storing harvested energy are assumed to be negligible. A lower storage efficiency can be modeled by scaling down the energy harvesting rate suitably.

B. Harvested Energy Usage

When a Relay i transmits, it does so at a constant power P_i, as has also been assumed in [1]–[4], [9].[1] Let α_i denote

[1]In [9], an analog delay line model was assumed for an AF relay. Therefore, the energy consumed by it was a function of the difference between the energy transmitted by it and energy input to it. In our model, the energy consumed by a relay is instead directly equal to the energy transmitted by it. This model is appropriate when the relay saves a digitally sampled version of the received signal, which is regenerated and amplified at the time of transmission. As in [9], the energy consumed by the transmit/receive circuitry is assumed to be negligible. This is justifiable when the transmission distances are relatively large; the energy transmitted is then the dominant source of energy consumption. The model can be refined further by also accounting for receive energy consumption and transmit circuit inefficiencies [23]. However, this is beyond the scope of this paper.

the signal amplification by Relay i if it were to transmit. It is chosen to ensure that the transmit power averaged over noise is P_i. Thus,

$$\alpha_i^2 = \frac{P_i}{P_s |h_{si}|^2 + N_0}, \quad (1)$$

where N_0 is the additive white Gaussian noise (AWGN) power. Thus, a relay inverts the effect of its SR link. For ease of notation, we assume the noise power to be the same for all nodes in the system; the analysis can be easily generalized to include non-identical noise powers at different receivers. The signal-to-noise-ratio (SNR) at the destination, γ_D, then equals [21]

$$\gamma_D = \gamma_0 + \frac{\gamma_{si}\gamma_{di}}{\gamma_{si} + \gamma_{id} + 1}, \quad (2)$$

where $\gamma_0 = |h_0|^2 \frac{P_s T_s}{N_0}$, $\gamma_{si} = |h_{si}|^2 \frac{P_s T_s}{N_0}$, and $\gamma_{di} = |h_{di}|^2 \frac{P_i T_s}{N_0}$. Let $\mathbf{E}[\gamma_0] = \bar{\gamma}_0$, $\mathbf{E}[\gamma_{si}] = \bar{\gamma}_{si}$, and $\mathbf{E}[\gamma_{di}] = \bar{\gamma}_{di}$, where $\mathbf{E}[.]$ denotes expectation.

In forwarding a symbol of duration T_s, a relay consumes an energy equal to $P_i T_s$. To forward a packet of δ symbols, the energy consumed is $P_i T_p$, where $T_p = \delta T_s$. A relay amplifies and forwards its received signal only if at least $P_i T_p$ energy is stored in its battery. Otherwise, it does not even receive the packet. A relay that has sufficient energy to transmit shall be said to be *active*. Note that an EH relay may be active or inactive at different time instants.

C. Energy Neutrality and Energy Constrained Relays

As mentioned, the energy availability at a relay is subject to the fundamental *energy neutrality* constraint, which mandates that the energy used by the relay thus far should not exceed the energy harvested by it. A key consequence of this is that a relay might not be active for some fraction of the time.

Let $\xi_i \geq 0$ denote the steady state probability that Relay i is active. Depending on ξ_i, we define the following two terms; these shall play a pivotal role in understanding the system behavior.

- *Energy unconstrained relay:* A Relay i is said to be energy unconstrained when $\xi_i = 1$.
- *Energy constrained relay:* A Relay i is said to be energy constrained when $\xi_i < 1$.

An energy unconstrained relay is, thus, always available for relaying. This occurs when the rate at which a relay harvests energy exceeds the average rate at which it consumes energy.

D. Relay Selection

As mentioned, when multiple active relays are available, *one* of them is selected to forward a packet. The symbol-error-rate (SER) is minimized when the relay that maximizes the end-to-end SNR of (2) is selected. We call this the *best relay selection* rule. In practice, selection can be implemented using a centralized polling mechanism or distributed mechanisms such as timer-based selection [7], [24] or splitting-based selection [25], [26]. The distributed mechanisms are fast and scale well as the number of relays increases. This is unlike the centralized polling mechanism in which the energy overhead increases linearly with N. In order to ensure analytical tractability and maintain focus on the impact of the energy harvesting on a cooperative network, we shall assume that the energy overhead of selection is negligible. The interested reader is referred to [27] for an analysis of the system-level performance tradeoffs associated with a selection mechanism.

III. SER Analysis: Symmetric Case

We shall focus on the SER of uncoded transmissions since it has been analyzed in several papers that deal with conventional AF relays [3]–[5], [8]. We consider MPSK constellations in this paper. The analysis can be generalized to MQAM constellations, as well.

We first develop expressions for the SER for the 'symmetric' case in which the SR channels are statistically identical, and so are the RD channels. Furthermore, the energy harvesting profile and the transmit powers of all relays are the same. The general case, in which the different channels and other relay parameters need not be identical, is considered next in Sec. IV.

Now, the S–i and i–D channel gains are i. i. d. with means $\bar{\gamma}_{si} = \bar{\gamma}_s$ and $\bar{\gamma}_{di} = \bar{\gamma}_d$, respectively. As before, the direct SD link has a mean gain of $\bar{\gamma}_0$. Also, $P_i = P$ and $E_i^{\text{av}} = E^{\text{av}}$ for all relays. It follows from symmetry that all relays have the same probability of being active, *i.e.*, $\xi_i = \xi$, for all i.

The energy stored in the battery of a Relay i clearly depends on how often it has been selected and how much energy it has harvested in the past and when. Consequently, the probability that the relay is active, ξ_i, is a function of the number of relays and the rate at which energy is harvested and used per transmission by a relay. The exact relationship is captured below.

Proposition 1: Let $\rho \triangleq \frac{2E^{\text{av}}}{P}$. The relays are energy constrained when $\rho < \frac{1}{N}$, in which case the probability that a relay is active, ξ, is

$$\xi = 1 - (1 - N\rho)^{\frac{1}{N}}. \quad (3)$$

All the relays are energy unconstrained ($\xi = 1$) when $\rho \geq \frac{1}{N}$.

Proof: The proof is relegated to Appendix A. A key enabler in the proof is a *decoupling* approximation, which assumes that the probability a relay node is active is independent of the probability of other relay nodes being active. It shall turn out to be accurate for all ρ. ■

The factor of 2 in $\rho = \frac{2E^{\text{av}}}{P}$ occurs because a node will harvest an average energy of $2E^{\text{av}}T_p$ in the two phases of the AF cooperation protocol. The dependency of ξ on N and ρ is clearly brought out by (3). As the product ρN increases, the probability that a relay is active increases, as expected. The above result also shows a key property of a voluntary EH relay system – *whether a relay is energy constrained or not depends on the other EH relays in the system.*

We now derive an expression for the fading-averaged end-to-end SER. The SER at any time depends on the subset of relays that are active. Due to symmetry, the SER conditioned on any one of the $\binom{N}{k}$ possible subsets of k active relays is the same. Hence, let SER_k denote the SER given that any k out of the total N relays are active. Let

$$\Lambda_i = \frac{\gamma_{si}\gamma_{di}}{\gamma_{si} + \gamma_{id} + 1} \approx \frac{\gamma_{si}\gamma_{di}}{\gamma_{si} + \gamma_{id}}. \quad (4)$$

The above approximation, which makes the analysis tractable, is accurate at larger values of γ_{si} and γ_{di} [4], [9], [22]. Let $f_{\Lambda_i}(.)$ and $F_{\Lambda_i}(.)$ denote the probability density function (PDF) and cumulative distribution function (CDF), respectively, of Λ_i for an arbitrary Relay i.

We treat the cases where $1 \leq k \leq N$ and $k = 0$ separately below.

Proposition 2: SER_k, for $1 \leq k \leq N$, can be written in terms of the PDF and CDF of Λ_i as

$$\text{SER}_k = k \int_0^\infty \psi(x) f_{\Lambda_i}(x) F_{\Lambda_i}^{k-1}(x)\, dx. \tag{5}$$

For $M = 2$ (BPSK),

$$\psi(x) = \frac{1}{2}\text{erfc}\left(\sqrt{x}\right) - \frac{1}{2}\exp\left(\frac{x}{\bar{\gamma}_0}\right)\frac{\text{erfc}\left(\sqrt{x\left(1+\frac{1}{\bar{\gamma}_0}\right)}\right)}{\sqrt{1+\frac{1}{\bar{\gamma}_0}}},$$

where erfc(.) is the complementary error function [28]. For $M > 2$, $\psi(x) = \psi_1(x) - \psi_2(x)$, where

$$\psi_1(x) = \text{erfc}\left(\sqrt{\frac{x}{\beta}}\right) - \exp\left(\frac{x}{\bar{\gamma}_0}\right)\frac{\text{erfc}\left(\sqrt{x\left(\beta+\frac{1}{\bar{\gamma}_0}\right)}\right)}{\sqrt{1+\frac{\beta}{\bar{\gamma}_0}}}, \tag{6}$$

and $\psi_2(x)$ is given by (7) at the top of the next page.

Proof: The proof is given in Appendix B. ∎

We have found that $r = 4$ is sufficient to compute (7) accurately. We now derive an accurate expression for SER_k.

Proposition 3: The SER given $k > 0$ relays are active is

$$\begin{aligned}&\text{SER}_k \\ &\approx k\sum_{n=0}^{W} w_n \left(\frac{4a_n\nu}{\mu^2}K_0\left(\frac{2a_n\sqrt{\nu}}{\mu}\right) + \frac{2a_n\sqrt{\nu}}{\mu}K_1\left(\frac{2a_n\sqrt{\nu}}{\mu}\right)\right) \\ &\times \psi\left(\frac{\nu}{\mu}a_n\right)\left(1 - \frac{2a_n\sqrt{\nu}}{\mu}K_1\left(\frac{2a_n\sqrt{\nu}}{\mu}\right)\exp\left(-a_n\right)\right)^{k-1},\end{aligned} \tag{8}$$

where $\nu = \bar{\gamma}_s\bar{\gamma}_d$, $\mu = \bar{\gamma}_s + \bar{\gamma}_d$, a_n and w_n, for $1 \leq n \leq W$, are the W Gauss-Laguerre abscissa and weights, respectively, and $K_l(\cdot)$ is the modified Bessel function of the second kind of order l [29]. When $k = 0$ relays are active,

$$\begin{aligned}\text{SER}_0 &= \frac{1}{2}\left(1 - \frac{1}{\sqrt{1+\beta/\bar{\gamma}_0}}\right) \\ &- \frac{1}{\pi}\left(\frac{\arctan\left(\sqrt{\beta-1}/\sqrt{1+\frac{\beta}{\bar{\gamma}_0}}\right)}{\sqrt{1+\frac{\beta}{\bar{\gamma}_0}}} - \arctan\left(\sqrt{\beta-1}\right)\right).\end{aligned} \tag{9}$$

Proof: The proof is relegated to Appendix C. ∎

The SER expression derived above, which is in a form that is analytically tractable for the EH relay system under consideration, is different from the expressions derived in [3], [5], [8] for conventional AF relays. In [8], a truncated Taylor series approximation for $K_0(x)$ and $K_1(x)$ was used. In [3], an approximation based on the probability of outage was used. In [5], Λ_i was lower bounded by $\frac{1}{2}\min\{\gamma_{si}, \gamma_{di}\}$. The various approaches are compared with our approach in Fig. 2, which plots the SER_k of BPSK from Monte Carlo simulations as a function of PT_s for $k = 4$ active relays. We observe that, compared to other approaches, our results are more accurate at lower SNR values and are just as accurate at high SNR values. We shall need this extra accuracy when we optimize the transmit power settings of the EH relays. The small difference between our analytical and simulation results for SNRs below 8 dB occurs because the analysis uses the approximation of (4), while the simulations do not. From Props. 1, 2, and 3, the final SER expression for a system with N EH relays is as follows.

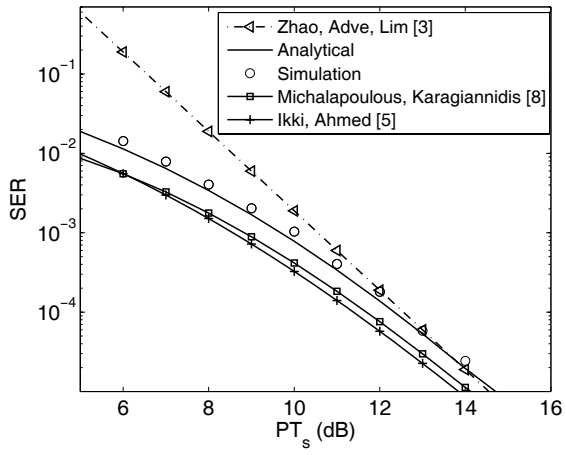

Fig. 2. Comparison of the analytical expression for SER_k in (8) with other approximations developed in the literature, for $P_sT_s = PT_s$ and $k = 4$ active relays.

Result *1:*

$$\begin{aligned}&\text{SER} \approx (1-\xi)^N \text{SER}_0 \\ &+ N\xi\sum_{n=0}^{W} w_n \left(\frac{4a_n\nu}{\mu^2}K_0\left(\frac{2a_n\sqrt{\nu}}{\mu}\right) + \frac{2a_n\sqrt{\nu}}{\mu}K_1\left(\frac{2a_n\sqrt{\nu}}{\mu}\right)\right) \\ &\times \psi\left(\frac{\nu}{\mu}a_n\right)\left(1 - \frac{2a_n\xi\sqrt{\nu}}{\mu}K_1\left(\frac{2a_n\sqrt{\nu}}{\mu}\right)\exp\left(-a_n\right)\right)^{N-1},\end{aligned} \tag{10}$$

where SER_0 is given by (9).

Proof: Unconditioning over the number of relays that are active, k, we get

$$\text{SER} = \sum_{k=1}^{N}\binom{N}{k}\xi^k(1-\xi)^{N-k}\text{SER}_k + (1-\xi)^N\text{SER}_0. \tag{11}$$

Substituting (3) and (8) in (11) and using combinatorial identities leads to (10). ∎

The above result holds in both energy constrained and unconstrained regimes and for any P_s and P. Note the dependence of the SER on the number of relays, N, and ρ. The latter depends on a relay's transmit power setting as well as its energy harvesting rate.

Energy unconstrained regime as a special case: In the energy unconstrained regime ($\xi = 1$), the SER is now the same as that of a conventional cooperative system with N available AF relays; this has been analyzed in [3], [5], [8].

$$\psi_2(x) = \sum_{r=0}^{\infty} \frac{A_r}{\beta^{r+\frac{1}{2}}} \left(x^{r+\frac{1}{2}} \Gamma\left(-\frac{1}{2}-r\right) + e^{-x} \frac{\Gamma(r+\frac{1}{2})}{\Gamma(r+\frac{3}{2})} {}_1F_1\left(1; \frac{1}{2}-r; x\right)\right) - \sum_{r=0}^{\infty} \frac{A_r a^r}{\beta^{r+\frac{1}{2}}} \exp\left(-\left(1+\frac{1}{\bar{\gamma}_0}\right)x + \frac{1}{\bar{\gamma}_0}\right)$$
$$\times \left(x^{r+\frac{1}{2}} e^{\left(1+\frac{1}{\bar{\gamma}_0}\right)x} \Gamma\left(-\frac{1}{2}-r\right) + \left(1+\frac{1}{\bar{\gamma}_0}\right)^{-r-\frac{1}{2}} \frac{\Gamma(r+\frac{1}{2})}{\Gamma(r+\frac{3}{2})} {}_1F_1\left(1; \frac{1}{2}-r; \left(1+\frac{1}{\bar{\gamma}_0}\right)x\right)\right), \quad (7)$$

where $A_r = \frac{1}{2\pi}\frac{1}{2^r r!}\prod_{j=1}^{r}(2j-1)$, $a = 1+\frac{\beta}{\bar{\gamma}_0}$, ${}_1F_1(.;.;.)$ is the confluent hyper-geometric function of a single variable, and $\Gamma(\cdot)$ is the Gamma function [28].

A. Asymptotic Analysis

Further insights about the impact of using EH relays on system performance can be gained by studying the following two asymptotic regimes.

1) Asymptotically Large N with $N\rho = \kappa$ Fixed: Here, the total energy harvested by all the relays remains constant as the number of relays increases. Only the energy constrained case of $\kappa < 1$ is relevant here.[2] In this case, the following key simplification occurs.

Proposition 4: The number of active relays follows a Poisson distribution with mean λ given by $\lambda = -\log_e(1-\kappa)$.

Proof: The proof is relegated to Appendix D. ∎

Using the above proposition in (11) and simplifying yields

$$\text{SER} = e^{-\lambda}\text{SER}_0 + \sum_{n=0}^{W} w_n \psi\left(\frac{\nu}{\mu}a_n\right)$$
$$\times \left(\frac{4a_n\nu}{\mu^2}K_0\left(\frac{2a_n\sqrt{\nu}}{\mu}\right) + \frac{2a_n\sqrt{\nu}}{\mu}K_1\left(\frac{2a_n\sqrt{\nu}}{\mu}\right)\right)$$
$$\times \exp\left(-\frac{2a_n\lambda\sqrt{\nu}}{\mu}K_1\left(\frac{2a_n\sqrt{\nu}}{\mu}\right)\exp\left(-a_n\right)\right), \quad (12)$$

where $\psi(x)$ is given in Prop. 2 and SER_0 is given in (9).

2) Asymptotically Large Mean Channel Gains ($\bar{\gamma}_0, \bar{\gamma}_{si}, \bar{\gamma}_{di} \to \infty$): In the energy constrained regime ($N\rho < 1$), as $\bar{\gamma}_0, \bar{\gamma}_{si}, \bar{\gamma}_{di} \to \infty$, the SER_0 term, which occurs due to the direct SD link, dominates in (10). This is because SER_k has a diversity order of $k+1$, for $1 \le k \le N$, and decays faster than SER_0, which has a diversity order of 1. Therefore, neglecting the higher order terms, the SER takes the following final form:

$$\text{SER} = (1-N\rho)\text{SER}_0,$$
$$\overset{(a)}{=} (1-N\rho)\left(\frac{1}{2} + \frac{1}{\pi}\arctan(\sqrt{\beta-1})\right)\frac{\beta}{2\bar{\gamma}_0}. \quad (13)$$

Here, (a) follows from (9) and shows only the dominant $1/\bar{\gamma}_0$ component.

In the energy unconstrained regime, $\text{SER} = \text{SER}_N$ since $\xi = 1$. Therefore, the diversity order becomes $N+1$, as in a conventional cooperative system with N relays [5], [8].

3) Implications of the Asymptotic Analysis: The asymptotic analysis helps understand the diversity order and energy gain benefits of using EH relays as follows.

- *Diversity order and energy gain*: From (13), we see that energy constrained relays do not improve the diversity order, which remains as 1. Note, however, that diversity order is a parameter defined for high SNR, which might not occur in an EH network for lower transmit power settings of the nodes and smaller mean channel gains. The $(1-N\rho)$ factor in (13) implies that the EH relays together provide an 'energy gain' of $-10\log_{10}(1-N\rho) > 0$ over direct SD transmission. The energy gain increases as $N\rho$ increases.
- *Combined case when $n \to \infty$ (with $N\rho = \kappa$ fixed) and $\bar{\gamma}_0, \bar{\gamma}_{si}, \bar{\gamma}_{di} \to \infty$:* As before, in the energy unconstrained regime, the diversity order is ∞. In the energy constrained regime ($\kappa < 1$), the SER expression in (12) simplifies to $\text{SER} = e^{-\lambda}\text{SER}_0 \overset{(b)}{=} (1-\kappa)\text{SER}_0$. Here, (b) follows from Prop. 4. The energy gain from using EH relays now equals $-10\log_{10}(1-\kappa)$ dB.

IV. Analysis: General Case With Asymmetric Channels

We now analyze the general case in which the various channels are independent but are not statistically identical. The relays can also transmit with different powers and harvest energies at different rates. Consequently, the probability, ξ_i, that Relay i is active depends on i. *Unlike the symmetric case, only a subset of the N relays may be energy constrained.* As before, let

$$\rho_i = \frac{2E_i^{\text{av}}}{P_i}. \quad (14)$$

Let $\mathcal{N} = \{1, \ldots, N\}$ denote the set of all the N relays. To evaluate the SER, we first need to determine the probabilities of different subsets of relays being active at any time instant.

A. Determining $\{\xi_i\}_{i=1}^{N}$ for Best Relay Selection

We first determine the probability that a Relay i is active. Let $\mathcal{U}$ be the set of U relays that are energy unconstrained. By definition, $\xi_j = 1$ for all $j \in \mathcal{U}$. Let $\mathcal{C} = \mathcal{N} \setminus \mathcal{U}$ denote the set of the remaining $N-U$ energy constrained relays.

Proposition 5: Given $\mathcal{U}$ and $\mathcal{C} = \mathcal{N} \setminus \mathcal{U} \neq \emptyset$ (null set), $\{\xi_i\}_{i\in\mathcal{C}}$ is the solution of the following set of $N-U$ multinomial equations that arise due to the energy neutrality condition. For $i \in \mathcal{C}$,

$$\rho_i = \xi_i \sum_{r=0}^{N-U-1} \binom{N-U-1}{r} \sum_{m=1}^{r+U} \sum_{l=0}^{r+U} (-1)^l \sum_{q=1}^{\binom{r+U}{l}} \left[\prod_{g\in\mathcal{C}_{m,i}^r} \xi_g\right]$$
$$\times \left[\prod_{j\in\mathcal{I}}(1-\xi_j)\right] \left(\frac{\bar{\gamma}_{si}+\bar{\gamma}_{di}}{\bar{\gamma}_{si}+\bar{\gamma}_{di}+\bar{\gamma}_{di}\bar{\gamma}_{si}\sum_{j\in\mathcal{L}_q^l}\frac{\bar{\gamma}_{s_j}+\bar{\gamma}_{d_j}}{\bar{\gamma}_{s_j}\bar{\gamma}_{d_j}}}\right), \quad (15)$$

[2] Otherwise, in the energy unconstrained regime, the number of active relays and, hence, the diversity order will be infinite.

where $\mathcal{C}_{m,i}^r$ is the mth subset of size r of the set $\mathcal{C} \setminus \{i\}$, $\mathcal{I} = \mathcal{C} \setminus \left(\mathcal{C}_{m,i}^r \cup \{i\}\right)$, and $\mathcal{L}_q^l$ is the qth subset of size l of the set $\mathcal{C}_{m,i}^r \cup \mathcal{U}$.

Proof: The proof is relegated to Appendix E. The extensive book keeping notation in (15) can be understood as follows. Excluding Relay i, $\mathcal{C}_{m,i}^r$ tracks the set of energy constrained relays that are active, $\mathcal{I}$ tracks the set of inactive relays, and $\mathcal{L}_q^l$ tracks the relays (including the energy unconstrained ones) that are active. ∎

From the equations above, it is clear that $\{\xi_i\}_{i=1}^N$ depend on N, $\{\bar{\gamma}_{si}\}_{i=1}^N$, $\{\bar{\gamma}_{di}\}_{i=1}^N$, and $\{\rho_i\}_{i=1}^N$. This is unlike the simpler symmetric case, where ξ_i depended on far fewer parameters. The above equations are solved numerically, e.g., using the function `fsolve` in MATLAB. However, they require the set of energy unconstrained relays, $\mathcal{U}$, as input. Next, we determine $\mathcal{U}$.

B. Determining the Set of Energy Unconstrained Relays, $\mathcal{U}$

In general, the set of unconstrained relays, $\mathcal{U} \subset \mathcal{N}$, can take one of 2^N values. It is determined by finding the subset for which the set of equations in (15) are self-consistent. However, a significant reduction in the search complexity occurs when either ρ_i or $\bar{\Lambda}_i$ is the same for all the relays. In this case, $\mathcal{U}$ can be only one of $N+1$ possible subsets. The reasoning behind this simplification is as follows.

Consider first the case where $\rho_i = \rho$, for all i. As $\bar{\Lambda}_i$ decreases for a Relay i, the relay gets selected less often and it consumes a smaller fraction of its harvested energy. Thus, if Relay i is energy unconstrained, then any Relay j for which $\bar{\Lambda}_j \leq \bar{\Lambda}_i$ would also be energy unconstrained. Therefore, $\mathcal{U}$ is created by successively including relays with larger $\bar{\Lambda}_i$ one by one until the set of equations in (15) becomes self-consistent. In fact, $\bar{\Lambda}_i$ can be written down in closed-form as $\bar{\Lambda}_i = \left(\frac{1}{\bar{\gamma}_{si}^2} - \frac{1}{\bar{\gamma}_{di}^2} + \frac{2}{\bar{\gamma}_{si}\bar{\gamma}_{di}} \log_e\left(\frac{\bar{\gamma}_{si}}{\bar{\gamma}_{di}}\right)\right)\left(\frac{1}{\bar{\gamma}_{si}} - \frac{1}{\bar{\gamma}_{di}}\right)^{-3}$, which makes it very easy to compute. The derivation follows from [9], and is not repeated here.

A similar procedure applies for the case when $\bar{\Lambda}_i$ is the same for all relays but ρ_is are not. In this case, $\mathcal{U}$ is created by successively including the relays one by one the in decreasing order of ρ_is until the set of equations in (15) becomes self-consistent. This is because if Relay i is unconstrained, then so would any Relay j for which $\rho_j \geq \rho_i$.

C. SER Analysis

Having determined $\{\xi i\}_{i=1}^N$, we can now evaluate the fading-averaged SER.

Result *2:* The SER for best relay selection is given by

$$\begin{aligned}\text{SER} = \text{SER}_0 &\left[\prod_{j=1}^{N}(1-\xi_j)\right] \\ &+ \sum_{n=1}^{W}\sum_{k=1}^{N}\sum_{m=1}^{\binom{N}{k}}\left[\prod_{j\in\mathcal{N}_m^k}\xi_j\right]\left[\prod_{h\in\mathcal{N}\setminus\mathcal{N}_m^k}(1-\xi_h)\right]\sum_{i\in\mathcal{N}_m^k} w_n \\ &\times\psi\left(\frac{\nu_i}{\mu_i}a_n\right)\left(\frac{4a_n\nu_i}{\mu_i^2}K_0\left(\frac{2a_n\sqrt{\nu_i}}{\mu_i}\right)+\frac{2a_n\sqrt{\nu_i}}{\mu_i}K_1\left(\frac{2a_n\sqrt{\nu_i}}{\mu_i}\right)\right) \\ &\times\prod_{j\in\mathcal{N}_m^k\setminus\{i\}}\left[1-\frac{2a_n\nu_i}{\mu_i\sqrt{\nu_j}}K_1\left(\frac{2a_n\nu_i}{\mu_i\sqrt{\nu_j}}\right)\exp\left(-\frac{\mu_j\nu_i}{\nu_j\mu_i}a_n\right)\right], \end{aligned} \tag{16}$$

where $\mathcal{N}_m^k$ denotes the mth subset of size k of $\mathcal{N}$.

Proof: The proof is relegated to Appendix F. ∎

The SER expression for the general case is more involved than in the symmetric case because the probability that a relay is selected depends not only on the number of active relays, but also which specific subset of relays is active.

D. Asymptotics

1) $N \to \infty$ with $\sum_{i=1}^N \rho_i$ Fixed: We do not delve into this case further as the expressions do not simplify significantly.

2) $\bar{\gamma}_{si}, \bar{\gamma}_{di}, \bar{\gamma}_0 \to \infty$: If all the N relays are energy constrained, then the SER expression in (16) reduces to $\text{SER} = \text{SER}_0 \prod_{j=1}^N (1-\xi_j)$. Therefore, the diversity order is still 1, as in the symmetric case. And, the energy gain from the EH relays equals $-10\sum_{j=1}^N \log_{10}(1-\xi_j)$ dB. When there are $U \geq 1$ energy unconstrained relays, the diversity order equals $U+1$. In such a case, we do not talk of an energy gain over direct SD transmission since the latter's diversity order of 1 is different from $U+1$.

V. Simulations and Discussion

We now study the analytical results graphically and also verify through Monte Carlo simulations, which use up to 10^6 samples, the accuracy of approximations that were made in the analysis. We first study the symmetric case in Sec. V-A and bring out the various inter-relationships and trade-offs associated with using EH relays in a cooperative system. The general case is studied thereafter in Sec. V-B. Unless mentioned otherwise, $N = 4$, $\delta = 25$ symbols (*i.e.*, $T_p = 25T_s$), and $N_0 = 1$. Simulation and analytical results are shown using markers (such as ∘) and lines, respectively. All results are reported in terms of the normalized energy consumed by a Relay i in transmitting a symbol, $P_i T_s$, and the average energy harvested by it in the two phases of the AF protocol, $2E_i^{\text{av}}T_p$.

A. Symmetric Case

We illustrate the results for $\mathbf{E}\left[|h_{si}|^2\right] = 1$ and $\mathbf{E}\left[|h_{di}|^2\right] = 1$. The SD link is weaker with $\mathbf{E}\left[|h_0|^2\right] = \frac{1}{4}$. Therefore, $\bar{\gamma}_{si} = P_s T_s$, $\bar{\gamma}_{di} = PT_s$, and $\bar{\gamma}_0 = \frac{P_s T_s}{4}$, where all relays transmit with the same power P.

Figure 3 plots the SER as a function of the MPSK constellation size, M, and the average energy harvested, $2E^{\text{av}}T_p$, when the energy consumed per symbol by the source and relays is $P_s T_s = PT_s = 10$ dB. As expected, the SER increases as M increases. As $2E^{\text{av}}T_p$ increases, the SER decreases instead. It eventually saturates once E^{av} exceeds $\frac{P}{2N}$ since all the relays become energy unconstrained. Now, the SER no longer depends on the energy harvesting parameters, and is entirely determined by the mean channel gains, P, and N.

Notice also in the figure that the simulation and analytical results match well. This verifies the combined accuracy of the following four approximations that were used in the analysis: (i) The decoupling approximation used in Prop. 1,

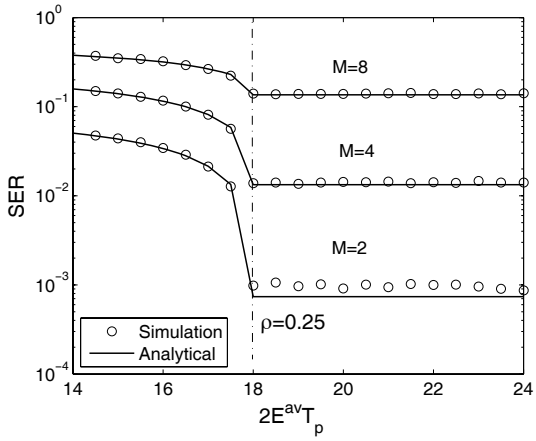

Fig. 3. SER as a function of the energy harvested ($2E^{\text{av}}T_p$) for different MPSK constellation sizes, M, when $PT_s = P_sT_s = 10$ dB.

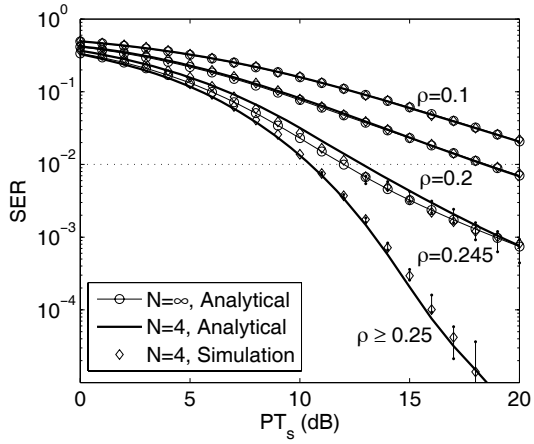

Fig. 4. SER as a function of the transmit energy per symbol (PT_s) for different values of ρ when $P_s = P$, QPSK, and $N = 4$ relays. For SER below 0.01, 99% confidence intervals are shown to demonstrate the relative accuracy of the Monte Carlo simulation results. For $\rho < 0.25$, also shown are results for the asymptotic case where $N \to \infty$ but with $\kappa = 4\rho$.

which assumes that the probability a relay node is active is independent of the probability of other relay nodes being active. Similar approximations have been used to good effect to analyze, for example, multiple access protocols [30] and mean field interaction models [31]. (ii) The noise term is ignored in the relay selection metric in (4). The accuracy of the approximation increases as the SNR increases. (iii) In Prop. 3, the definite integral in (8) is approximated with a summation of W Gauss-Laguerre quadrature terms. Setting $W = 8$ suffices to get accurate results. (iv) In (7), the convergent series expansion of $\psi_2(x)$ is truncated. We have found 4 terms to be sufficient to get numerically accurate results.

Figure 4 plots the SER as a function of the energy spent per symbol by a relay, PT_s, for four different values of ρ. When $\rho < \frac{1}{N} = 0.25$, the relays are energy constrained and the diversity order of the system is 1. Therefore, the three SER curves for $\rho < 0.25$ become parallel to each other for large PT_s. When $\rho \geq 0.25$, all the relays are energy unconstrained. This makes the diversity order increase to $N + 1 = 5$, and is reflected in the steeper slope for the corresponding curve. Note, however, that the different diversity orders visibly manifest themselves only when $PT_s > 10$ dB. Also plotted for each $\rho < 0.25$ curve is the analytical SER result, from (12), for asymptotically large N with $\kappa = 4\rho$. We observe that the asymptotic results, despite their analytical simplicity, are good approximations even when N is as small as four.

We now investigate how the relay transmission energy should be set as a function of the energy harvesting rate in order to minimize the SER. This is done in Fig. 5, which plots the SER as a function of PT_s when $2E^{\text{av}}T_p = 20$ dB and 26 dB. When $2E^{\text{av}}T_p$ increases from 20 dB to 26 dB, the optimum value of PT_s, which is determined numerically, increases from 12 dB to 18 dB. The curves can be understood as follows. For $P < 2E^{\text{av}}/N$, all the relays are energy unconstrained, which makes the two curves coincide for small PT_s. As PT_s increases, the SER decreases as expected. However, once PT_s exceeds $2NE^{\text{av}}T_s$, all the relays become energy constrained. Therefore, the SER becomes sensitive to $2E^{\text{av}}T_p$, and increases as PT_s increases. For large PT_s, since the relays are inactive for most of the time, the SER gets

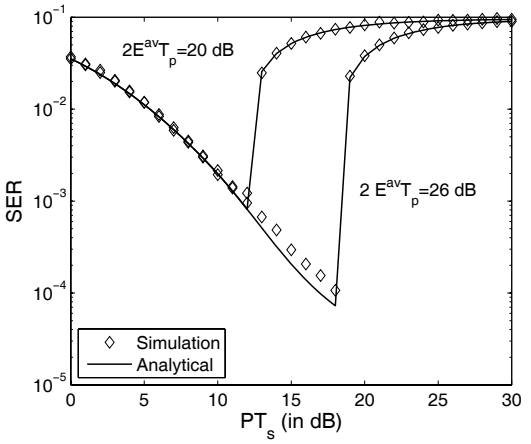

Fig. 5. Effect of relay transmit energy per symbol (PT_s) on SER as a function of the average energy harvested by a relay, when $P_sT_s = 15$ dB, QPSK, and $N = 4$ relays.

determined primarily by the SD channel and is dependent only on P_sT_s.

The optimal transmit power setting as a function of E^{av} is investigated further in Fig. 6, which plots the SER as a function of $2E^{\text{av}}T_p$ for different values of PT_s. Also plotted is the lower hull of the above curves. We observe from the plot that the optimal value of P is $2NE^{\text{av}}$, in which case $\rho = \frac{1}{N}$. *Thus, the optimum power setting ensures that the relays have just entered the energy unconstrained regime.* In effect, the EH relays should transmit with as high an energy as possible while remaining energy unconstrained.

B. General Case of Asymmetric Channels

We now study the general case in which the various mean channel gains are different. This is illustrated by setting $\mathbf{E}\left[|h_{si}|^2\right] = \mathbf{E}\left[|h_{di}|^2\right] = \frac{1}{2^{i-1}}$, for $1 \leq i \leq 4$. As before, $\mathbf{E}\left[|h_0|^2\right] = \frac{1}{4}$. For ease of illustration, we set $E_i^{\text{av}} = E^{\text{av}}$ and $P_i = P$ for all relays.

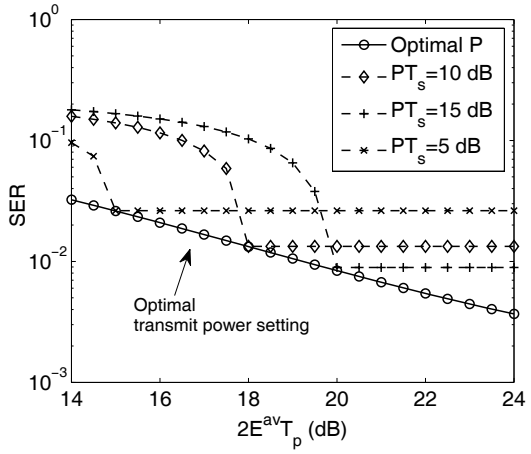

Fig. 6. Determining the optimal relay transmit energy (PT_s) as a function of E^{av}, when $P_sT_s = 10$ dB, QPSK, and $N = 4$ relays.

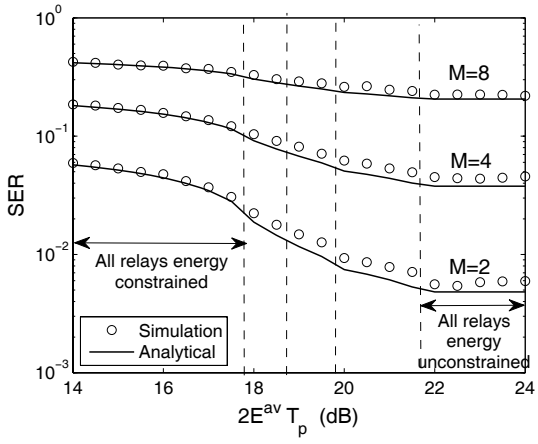

Fig. 7. General asymmetric case: SER *vs.* $2E^{\text{av}}T_p$, when $P_sT_s = PT_s = 16$ dB, QPSK, and $N = 4$ relays.

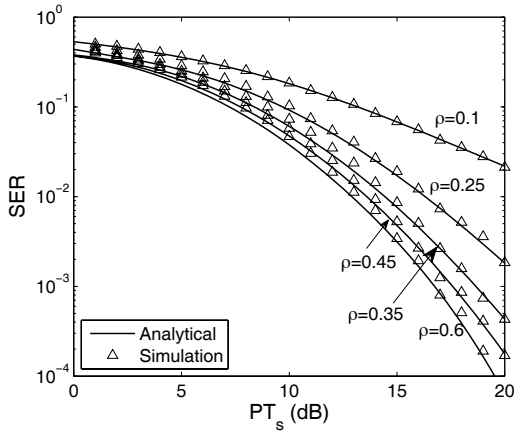

Fig. 8. General asymmetric case: SER *vs.* PT_s as a function of ρ, when $P_sT_s = PT_s$, QPSK, and $N = 4$ relays. All relays are energy constrained for $\rho = 0.1$. When $\rho = 0.25$, Relay 4 is energy unconstrained. When $\rho = 0.35$, Relays 3 and 4 are energy unconstrained. When $\rho = 0.45$, Relays 2, 3, and 4 are energy unconstrained. Finally, when $\rho = 0.6$, all four relays are energy unconstrained.

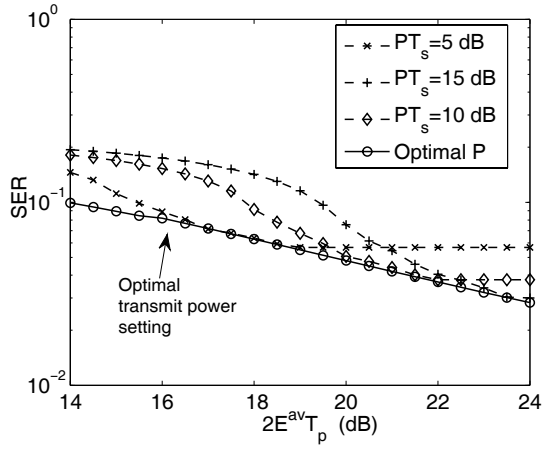

Fig. 9. General asymmetric case: SER *vs.* $2E^{\text{av}}T_p$ for different transmit power settings PT_s, and determination of the optimal transmit power setting (QPSK and $N = 4$).

Figure 7 plots the SER as a function of E^{av} for different constellation sizes. It is analogous to Fig. 3 for the symmetric case, and brings out the following additional points. As E^{av} increases, different relays become energy unconstrained at different E^{av} values. All relays are energy constrained for $\rho = 0.1$. Relay 4, which has the weakest RD channel and is selected the least often among all the relays, is the first to become energy unconstrained once $\rho \geq 0.25$, *i.e.*, $2E^{\text{av}}T_p \geq 18$ dB. Similarly, Relays 3 and 2 become unconstrained at $\rho \geq 0.3$ (*i.e.*, $2E^{\text{av}}T_p \geq 19$ dB) and $\rho \geq 0.4$ (*i.e.*, $2E^{\text{av}}T_p \geq 20$ dB), respectively. At $\rho = 0.6$ (*i.e.*, $2E^{\text{av}}T_p = 22$ dB), all the four relays are energy unconstrained.

Figure 8 plots the SER as a function of PT_s, for different ρ. The values of ρ are chosen so that a different number of relays is unconstrained for each ρ. As in Fig. 7, when $\rho = 0.1$, all the four relays are energy constrained and the diversity order of system is 1. When $\rho = 0.25$, Relay 4 is unconstrained, which increases the diversity order to 2, and so on. This behavior is different from the symmetric case, where the diversity order was either 1 or $N + 1$.

In Fig. 9, we determine the optimal transmit power setting. The SER is plotted as a function of $2E^{\text{av}}T_p$ for different PT_s. As in the symmetric case, we observe that the optimal PT_s is such that all the relays are energy unconstrained and one relay has just become energy unconstrained.

VI. Conclusions

We investigated the benefits of using energy harvesting nodes as amplify-and-forward cooperative relays that can perpetually assist conventional source and destination nodes to communicate with each other. We introduced the notion of energy constrained and energy unconstrained relays. For a general class of energy harvesting profiles, we derived closed-form expressions for the SER of the system and the asymptotic energy savings at the source from the use of EH relays. The analysis was made tractable by an accurate decoupling approximation about the energy availability at the relays.

A key observation about the system that follows from the analysis is that the energy harvesting profile influences system performance through a single parameter, namely, the average rate at which each node harvests energy. Whether a relay is

energy constrained or not depends not only on the average rate at which its harvests energy, but also on its transmit power and the total number of relays in the system.

Altogether, an EH cooperative relay system differs from the conventional relay system in several respects, and offers a promising way of improving performance. One important application for EH relays is wireless sensor networks, which are often energy constrained. Our results motivate several ideas for future research such as improving the relay selection rule to also account for the relay's battery state. Another interesting extension is a system in which the source and the destination nodes also harvest energy.

APPENDIX

A. Proof of Prop. 1

First consider the case where the relays are energy constrained, *i.e.*, a relay consumes all the energy it harvests. Let $\Pr(\text{Relay } i \text{ sel.})$ denote the probability that Relay i is selected (sel.). From the energy neutrality constraint and the ergodicity and stationarity of the energy harvesting process, we have

$$\rho = \frac{2E^{\text{av}}T_p}{PT_p} = \Pr(\text{Relay } i \text{ sel.}). \tag{17}$$

Since only an active relay is selected, $\Pr(\text{Relay } i \text{ sel.}) = \Pr(\text{Relay } i \text{ active}, \text{Relay } i \text{ sel.})$. Hence,

$$\begin{aligned}&\Pr(\text{Relay } i \text{ sel.})\\ &= \sum_{r=0}^{N-1} \Pr(\text{Relay } i \text{ sel.}|\text{Relay } i \text{ active}, r \text{ other active relays})\\ &\qquad \times \Pr(R_i \text{ is active}, r \text{ other active relays}).\end{aligned} \tag{18}$$

We now make the *decoupling* approximation that the event that a relay node is active is independent of whether other relay nodes are active or not. Hence,

$$\begin{aligned}&\Pr(\text{Relay } i \text{ active}, r \text{ other active relays})\\ &\qquad \approx \xi \binom{N-1}{r} \xi^r (1-\xi)^{N-1-r}.\end{aligned} \tag{19}$$

From symmetry, we can observe for any r that $\Pr(\text{Relay } i \text{ sel.}|\text{Relay } i \text{ active}, r \text{ other active relays}) = 1/(r+1)$. Thus,

$$\rho = \xi \sum_{k=0}^{N-1} \frac{1}{r+1} \binom{N-1}{r} \xi^r (1-\xi)^{N-r-1} = \frac{1-(1-\xi)^N}{N}.$$

Rearranging terms yields (3). The derivation above also shows that $\rho N < 1$ when $\xi < 1$. When $\xi = 1$, the system harvests more energy than it can use. Therefore, $\rho N \geq 1$.

B. Proof of Prop. 2

From (2), $\gamma_D = \gamma_0 + \Lambda_{[1]}$, where $\Lambda_{[1]} \triangleq \max_i \Lambda_i$. Recall from (4) that $\Lambda_i \approx \frac{\gamma_{si}\gamma_{di}}{\gamma_{si}+\gamma_{di}}$. From [32], SER_k for MPSK takes the form

$$\text{SER}_k = \frac{1}{\pi} \int_0^{\frac{M-1}{M}\pi} \mathcal{M}_{\gamma_D}\left(-\frac{\sin^2(\pi/M)}{\sin^2(\phi)}\right) d\phi, \tag{20}$$

where $\mathcal{M}_{\gamma_D}(s)$ is the moment generating function (MGF) of γ_D. Since the SD link is independent of the SR and RD links, we have $\mathcal{M}_{\gamma_D}(s) = \mathcal{M}_{\gamma_0}(s)\mathcal{M}_{\Lambda_{[1]}}(s)$. Since γ_0 is exponentially distributed with mean $\bar{\gamma}_0$, $\mathcal{M}_{\gamma_0}(s) = \frac{1}{1-\bar{\gamma}_0 s}$. Furthermore, the PDF of $\Lambda_{[1]}$ is $f_{\Lambda_{[1]}} = k f_{\Lambda_i}(x) F_{\Lambda_i}^{k-1}(x)$ [33]. Therefore, $\mathcal{M}_{\Lambda_{[1]}}(s) = \int_0^\infty k f_{\Lambda_i}(x) F_{\Lambda_i}(x)^{k-1} e^{-sx}\, dx$ and

$$\begin{aligned}\text{SER}_k = \frac{1}{\pi} \int_0^{\frac{M-1}{M}\pi} \int_0^\infty &\frac{1}{1+\bar{\gamma}_0\left(\frac{\sin^2(\pi/M)}{\sin^2(\phi)}\right)} k f_{\Lambda_i}(x) F_{\Lambda_i}^{k-1}(x)\\ &\times \exp\left(-x\frac{\sin^2(\pi/M)}{\sin^2(\phi)}\right) dx\, d\phi.\end{aligned} \tag{21}$$

Equivalently, $\text{SER}_k = \int_0^\infty \psi(x) k f_{\Lambda_i}(x) F_{\Lambda_i}^{k-1}(x)\, dx$, where $\psi(x) = \frac{1}{\pi}\int_0^{\frac{M-1}{M}\pi} \frac{\exp\left(-\frac{x}{\beta \sin^2(\phi)}\right)}{1+\frac{\bar{\gamma}_0}{\beta \sin^2(\phi)}}\, d\phi$.

1) Evaluation of $\psi(x)$ for BPSK: For BPSK we have, $\psi(x) = \frac{1}{\pi}\int_0^{\frac{\pi}{2}} \frac{\exp\left(-\frac{x}{\sin^2(\phi)}\right)}{1+\frac{\bar{\gamma}_0}{\sin^2(\phi)}}\, d\phi$. Using the variable substitution $\csc^2(\phi) = t^2+1$ and simplifying, we can show that

$$\psi(x) = \frac{e^{-x}}{\pi}\int_0^\infty \frac{e^{-xt^2}}{t^2+1} dt - \frac{e^{-x}}{\pi}\int_0^\infty \frac{e^{-xt^2}}{t^2+1+\frac{1}{\bar{\gamma}_0}}\, dt. \tag{22}$$

Using the identity in [28, (3.466.1)] yields the desired expression for $\psi(x)$ for BPSK.

2) Evaluation of $\psi(x)$ for MPSK ($M > 2$): For $M > 2$, $\frac{\pi}{2} < \frac{(M-1)}{M}\pi < \pi$. Therefore,

$$\begin{aligned}\psi(x) = \frac{1}{\pi}\int_0^{\frac{\pi}{2}} &\frac{e^{-\left(\frac{x}{\beta \sin^2(\phi)}\right)}}{1+\frac{\bar{\gamma}_0}{\beta \sin^2(\phi)}}\, d\phi\\ &+ \frac{1}{\pi}\int_{\frac{\pi}{2}}^{\left(\frac{M-1}{M}\right)\pi} \frac{e^{-\left(\frac{x}{\beta \sin^2(\phi)}\right)}}{1+\frac{\bar{\gamma}_0}{\beta \sin^2(\phi)}}\, d\phi.\end{aligned} \tag{23}$$

Substituting $\csc^2(\phi) = y$ in (23) results in

$$\begin{aligned}\psi(x) = &\underbrace{\frac{1}{\pi}\int_1^\infty \frac{e^{-y\frac{x}{\beta}}}{y\sqrt{y-1}\left(1+y\frac{\bar{\gamma}_0}{\beta}\right)} dy}_{\psi_1(x)}\\ &- \underbrace{\frac{1}{2\pi}\int_\beta^\infty \frac{e^{-y\frac{x}{\beta}}}{y\sqrt{y-1}\left(1+y\frac{\bar{\gamma}_0}{\beta}\right)} dy}_{\psi_2(x)}.\end{aligned} \tag{24}$$

The evaluation of the first integral, $\psi_1(x)$, is similar to that for BPSK done before. To evaluate the second integral, $\psi_2(x)$, we take a partial fraction expansion of its integrand to get

$$\begin{aligned}\psi_2(x) = \frac{1}{2\pi}\int_\beta^\infty &\frac{e^{-y\frac{x}{\beta}}}{y\sqrt{y-1}} dy\\ &- \frac{1}{2\pi}\int_\beta^\infty \frac{e^{-y\frac{x}{\beta}}}{\sqrt{y-1}\left(y+\frac{\beta}{\bar{\gamma}_0}\right)} dy,\end{aligned} \tag{25}$$

where $\beta = \csc^2(\pi/M) > 1$ since $M > 2$. Taking the Taylor series expansion of $(1-1/y)^{-1/2}$, we can show that the first term of (25) evaluates to $\sum_{r=0}^\infty A_r \int_\beta^\infty \frac{1}{y^{r+3/2}} e^{-y\frac{x}{\beta}}\, dy$, where

A_r is as defined in Prop. 2.[3] The integrals in the summation further simplify using the identity in [28, (3.381.6)]. The second term of (25) can be simplified similarly to obtain (7).

C. Proof of Prop. 3

For $1 \leq k \leq N$*:* The CDF $F_{\Lambda_i}(x)$ and PDF $f_{\Lambda_i}(x)$ of Λ_i are given by [4]: $F_{\Lambda_i}(x) = 1 - \frac{2x}{\sqrt{\nu}} K_1\left(\frac{2x}{\sqrt{\nu}}\right) \exp\left(-\frac{\mu}{\nu}x\right)$ and $f_{\Lambda_i}(x) = \left(\frac{4x}{\nu} K_0\left(\frac{2x}{\sqrt{\nu}}\right) + \frac{2x\mu}{\nu\sqrt{\nu}} K_1\left(\frac{2x}{\sqrt{\nu}}\right)\right) \exp\left(-\frac{\mu}{\nu}x\right)$. Substituting the PDF and CDF expressions in (5) and using the variable transformation $z = \frac{\mu}{\nu}x$, we get

$$\mathrm{SER}_k = k \int_0^\infty \left(\frac{4z\nu}{\mu} K_0\left(\frac{2z\sqrt{\nu}}{\mu}\right) \frac{2z\sqrt{\nu}}{\mu} K_1\left(\frac{2z\sqrt{\nu}}{\mu}\right)\right) \times \left(1 - \frac{2z\sqrt{\nu}}{\mu} K_1\left(\frac{2z\sqrt{\nu}}{\mu}\right) \exp(-z)\right)^{k-1} \psi\left(\frac{\nu}{\mu}z\right) \exp(-z) dz. \tag{26}$$

The final expression in (8) follows by using Gauss-Laguerre quadrature with the integration order as W [29].

For $k = 0$*:* Now, only the direct SD Rayleigh fading link matters. Therefore, $\mathrm{SER}_0 = \frac{1}{\pi} \int_0^{\left(\frac{M-1}{M}\right)\pi} \frac{1}{1 + \bar{\gamma}_0 \frac{\sin^2(\pi/M)}{\sin^2(\phi)}} d\phi$. This, upon simplifying, yields (9).

D. Proof of Prop. 4

From (19), the number of relays out of N EH relays that are active is binomially distributed. As $N \to \infty$, it can be easily shown that $\lim_{N\to\infty} \binom{N}{k} \xi^k (1-\xi)^{N-k} = \exp(-\lambda)\frac{\lambda^k}{k!}$, where

$$\lambda = \lim_{N\to\infty} N\xi \overset{(a)}{=} \lim_{N\to\infty} \frac{1 - (1-\kappa)^{1/N}}{1/N} = -\log_e(1-\kappa). \tag{27}$$

Here, (a) follows from Prop. 1.

E. Proof of Prop. 5

For an energy unconstrained Relay $j \in \mathcal{U}$, we have by definition $\xi_j = 1$. As in the symmetric case, the stationarity and ergodicity of the energy harvesting process and the energy neutrality condition imply that $\rho_i = \Pr(\text{Relay } i \text{ sel.})$ for an energy constrained Relay i. Let $\mathcal{C}^r_{m,i}$ be the mth *active subset of size* r of the set $\mathcal{N} \setminus (\mathcal{U} \cup \{i\}) = \mathcal{C} \setminus \{i\}$. Conditioning on various subsets $\mathcal{C}^r_{m,i}$, we get the following from the law of total probability:

$$\rho_i = \Pr(\text{Relay } i \text{ sel.}) = \sum_{r=0}^{N-U-1} \sum_{m=1}^{\binom{N-U-1}{r}} \Pr(\text{Relay } i \text{ sel.} | \{i\} \cup \mathcal{C}^r_{m,i} \cup \mathcal{U} \text{ are active}) \times \Pr(\{i\} \cup \mathcal{C}^r_{m,i} \cup \mathcal{U} \text{ are active}). \tag{28}$$

[3]The integral and summation can be swapped because the series $\sum_{r=0}^\infty A_r \frac{1}{y^{r+3/2}} e^{-y\frac{x}{\beta}}$ is dominated for all $y \in [\beta, \infty)$ by the absolutely convergent series $\sum_{r=0}^\infty A_r \frac{1}{\beta^{r+3/2}} e^{-x}$ [34].

As in the symmetric case, the decoupling approximation implies that

$$\Pr(\{i\} \cup \mathcal{C}^r_{m,i} \cup \mathcal{U} \text{ are active}) = \xi_i \left[\prod_{l \in \mathcal{C}^r_{m,i}} \xi_l\right] \left[\prod_{j \in \mathcal{I}} (1 - \xi_j)\right], \tag{29}$$

where $\mathcal{I} = \mathcal{N} \setminus \left(\{i\} \cup \mathcal{C}^r_{m,i} \cup \mathcal{U}\right) = \mathcal{C} \setminus \left(\{i\} \cup \mathcal{C}^r_{m,i}\right)$.

We now determine $\Pr(\text{Relay } i \text{ sel.} | \{i\} \cup \mathcal{C}^r_{m,i} \cup \mathcal{U} \text{ are active})$ as follows. Let $\mathcal{L} = \mathcal{C}^r_{m,i} \cup \mathcal{U}$. Then,

$$\Pr(\text{Relay } i \text{ sel.} | \mathcal{L} \cup \{i\} \text{ are active}) = \mathbf{E}\left[\Pr\left(\Lambda_i > \max_{j \in \mathcal{L}} \Lambda_j | \gamma_{si}, \gamma_{di}\right)\right]. \tag{30}$$

While a closed-form answer for the above integral is analytically intractable, the approximation $\Lambda_j \approx \min(\gamma_{sj}, \gamma_{dj})$ circumvents this problem [9]; it is tight when γ_{si} and γ_{di} are different. Then,

$$\Pr(\text{Relay } i \text{ sel.} | \mathcal{L} \cup \{i\} \text{ are active}) \approx \int_0^\infty \int_0^x \prod_{j \in \mathcal{L}} \left[1 - \exp\left(-\frac{\mu_j}{\nu_j} y\right)\right] f_{\gamma_{di}}(y) f_{\gamma_{si}}(x)\, dy dx + \int_0^\infty e^{-\frac{x}{\bar{\gamma}_{di}}} \prod_{j \in \mathcal{L}} \left[1 - \exp\left(-\frac{\mu_j}{\nu_j} x\right)\right] f_{\gamma_{si}}(x)\, dx. \tag{31}$$

Expanding the integrands above as a sum of various exponentials and simplifying, we get

$$\Pr(\text{Relay } i \text{ sel.} | \mathcal{L} \cup \{i\} \text{ are active}) \approx \sum_{l=0}^{r+U} (-1)^l \sum_{q=1}^{\binom{r+U}{l}} \frac{\bar{\gamma}_{si} + \bar{\gamma}_{di}}{\bar{\gamma}_{si} + \bar{\gamma}_{di} + \bar{\gamma}_{di}\bar{\gamma}_{si} \sum_{j \in \mathcal{L}^l_q} \frac{\bar{\gamma}_{s_j} + \bar{\gamma}_{d_j}}{\bar{\gamma}_{s_j}\bar{\gamma}_{d_j}}}, \tag{32}$$

where $\mathcal{L}^l_q$ is the qth subset of size l of the set $\mathcal{L}$, whose cardinality is $r + U$.[4] Substituting (29) and (32) in (28) yields (15).

F. Proof of Result 2

Using the MGF-based approach of Appendix B, $\mathrm{SER}_{\mathcal{C}^k_m}$, which denotes the SER given that $\mathcal{C}^k_m$ is the set of active relays, can be written as $\mathrm{SER}_{\mathcal{C}^k_m} = \sum_{i \in \mathcal{C}^k_m} \int_0^\infty \psi(x) f_{\Lambda_i}(x) \left[\prod_{j \in \mathcal{C}^k_m \setminus \{i\}} F_{\Lambda_j}(x)\right] dx$, where $f_{\Lambda_i}(x)$ and $F_{\Lambda_i}(x)$ denote the PDF and CDF, respectively, of Λ_i. Here, $\Lambda_i = \frac{\gamma_{si}\gamma_{di}}{\gamma_{si} + \gamma_{id}}$ (from (4)) and $\psi(x)$ for BPSK and MPSK is given in Prop. 2. The final SER expression is obtained by unconditioning over all the possible subsets. These subsets now occur with different probabilities, which are calculated using Prop. 5.

ACKNOWLEDGMENT

The authors would like to thank Chandra R. Murthy (IISc) for technical discussions and for his valuable comments on a preliminary draft of this paper.

[4]Note that the case of $\mathcal{L} = \mathcal{N} \setminus \{i\}$, which was considered in [9], is a special case of the above general result.

REFERENCES

[1] J. N. Laneman, D. N. C. Tse, and G. W. Wornell, "Cooperative diversity in wireless networks: efficient protocols and outage behavior," *IEEE Trans. Inf. Theory*, vol. 50, pp. 3062–3080, 2004.

[2] M. O. Hasna and M.-S. Alouini, "End-to-end performance of transmission systems with relays over Rayleigh-fading channels," *IEEE Trans. Wireless Commun.*, vol. 2, pp. 1126–1131, Nov. 2003.

[3] Y. Zhao, R. Adve, and T. J. Lim, "Symbol error rate of selection amplify-and-forward relay systems," *IEEE Commun. Lett.*, vol. 10, pp. 757–759, Nov. 2006.

[4] P. A. Anghel and M. Kaveh, "Exact symbol error probability of a cooperative network in a Rayleigh-fading environment," *IEEE Trans. Wireless Commun.*, vol. 3, pp. 1416–1421, Sep. 2004.

[5] S. S. Ikki and M. H. Ahmed, "Performance analysis of generalized selection combining for amplify-and-forward cooperative-diversity networks," in *Proc. ICC*, 2009.

[6] D. S. Michalopoulos and G. K. Karagiannidis, "Two-relay distributed switch and stay combining (DSSC)," *IEEE Trans. Commun.*, vol. 56, pp. 1790–1794, Nov. 2008.

[7] A. Bletsas, A. Khisti, D. P. Reed, and A. Lippman, "A simple cooperative diversity method based on network path selection," *IEEE J. Sel. Areas Commun.*, vol. 24, pp. 659–672, Mar. 2006.

[8] D. S. Michalopoulos and G. K. Karagiannidis, "Performance analysis of single relay selection in Rayleigh fading," *IEEE Trans. Wireless Commun.*, vol. 7, pp. 3718–3724, Oct. 2008.

[9] D. S. Michalopoulos and G. K. Karagiannidis, "PHY-layer fairness in amplify and forward cooperative diversity systems," *IEEE Trans. Wireless Commun.*, vol. 7, pp. 1073–1083, Mar. 2008.

[10] T. Himsoon, W. P. Siriwongpairat, Z. Han, and K. J. R. Liu, "Lifetime maximization via cooperative nodes and relay deployment in wireless networks," *IEEE J. Sel. Areas Commun.*, vol. 25, pp. 306–317, Feb. 2007.

[11] A. Kansal, J. Hsu, S. Zahedi, and M. B. Srivastava, "Power management in energy harvesting sensor networks," *ACM Trans. Embedded Comput. Syst.*, vol. 7, pp. 1–38, Sep. 2007.

[12] C. R. Murthy, "Power management and data rate maximization in wireless energy harvesting sensors," *Intl. J. Wireless Inf. Netw.*, July 2009.

[13] F. Simjee and P. H. Chou, "Everlast: long-life, supercapacitor-operated wireless sensor node," in *Proc. Intl. Symp. Low Power Electronics and Design*, pp. 197–202, 2006.

[14] J. A. Paradiso and T. Starner, "Energy scavenging for mobile and wireless electronics," *IEEE Trans. Pervasive Comput.*, pp. 18–27, Jan.–Mar. 2005.

[15] V. Raghunathan, S. Ganeriwal, and M. Srivastava, "Emerging techniques for long lived wireless sensor networks," *IEEE Commun. Mag.*, pp. 108–114, Apr. 2006.

[16] B. Medepally, N. B. Mehta, and C. R. Murthy, "Implications of energy profile and storage on energy harvesting sensor link performance," in *Proc. Globecom*, 2009.

[17] J. Lei, R. Yates, and L. Greenstein, "A generic model for optimizing single-hop transmission policy of replenishable sensors," *IEEE Trans. Wireless Commun.*, vol. 8, pp. 547–551, Feb. 2009.

[18] D. Niyato, E. Hossain, and A. Fallahi, "Sleep and wakup strategies in solar-powered wireless sensor/mesh networks: Performance analysis and optimization," *IEEE Trans. Mobile Comput.*, vol. 6, pp. 221–236, Feb. 2007.

[19] S. Ikki, M. H. Ahmed, and M. Uysal, "On the performance of adaptive decode-and-forward cooperative diversity with the nth best-relay selection scheme," in *Proc. Globecom*, Nov. 2009.

[20] M. Tacca, P. Monti, and A. Fumagalli, "Cooperative and reliable ARQ protocols for energy harvesting wireless sensor nodes," *IEEE Trans. Wireless Commun.*, vol. 6, pp. 2519–2529, July 2007.

[21] A. Ribeiro, X. Cai, and G. B. Giannakis, "Symbol error probabilities for general cooperative links," *IEEE Trans. Wireless Commun.*, vol. 4, pp. 1264–1273, May 2005.

[22] D. S. Michalopoulos, G. K. Karagiannidis, T. A. Tsiftsis, and R. K. Mallik, "Distributed transmit antenna selection (DTAS) under performance or energy consumption constraints," *IEEE Trans. Wireless Commun.*, vol. 7, pp. 1168–1173, Apr. 2008.

[23] S. Cui, A. J. Goldsmith, and A. Bahai, "Energy-constrained modulation optimization," *IEEE Trans. Wireless Commun.*, vol. 4, pp. 2349–2360, 2005.

[24] V. Shah, N. B. Mehta, and R. Yim, "Optimal timer based selection schemes," *IEEE Trans. Commun.*, vol. 58, pp. 1814–1823, June 2010.

[25] X. Qin and R. Berry, "Opportunistic splitting algorithms for wireless networks," in *Proc. INFOCOM*, pp. 1662–1672, Mar. 2004.

[26] V. Shah, N. B. Mehta, and R. Yim, "Splitting algorithms for fast relay selection: generalizations, analysis, and a unified view," *IEEE Trans. Wireless Commun.*, vol. 9, pp. 1525–1535, Apr. 2010.

[27] V. Shah, N. B. Mehta, and R. Yim, "The relay selection and transmission tradeoff in cooperative communication systems," *IEEE Trans. Wireless Commun.*, vol. 9, pp. 2505–2515, Aug. 2010.

[28] I. S. Gradshteyn and I. M. Ryzhik, *Table of Integrals, Series and Products*, 4th edition. Academic Press, 1980.

[29] M. Abramowitz and I. Stegun, *Handbook of Mathematical Functions with Formulas, Graphs, and Mathematical Tables*, 9th edition. Dover, 1972.

[30] G. Bianchi, "Performance analysis of IEEE 802.11 distributed coordination function," *IEEE J. Sel. Areas Commun.*, vol. 18, pp. 535–547, Mar. 2000.

[31] M. Benaim and J.-Y. L. Boudec, "A class of mean field interaction models for computer and communication systems," *Perform. Eval.*, vol. 65, pp. 823–838, Nov. 2008.

[32] M. K. Simon and D. Divsalar, "Some new twists to problems involving the Gaussian probability integral," *IEEE Trans. Commun.*, vol. 46, pp. 200–210, Feb. 1998.

[33] H. A. David and H. N. Nagaraja, *Order Statistics*, 3rd edition. Wiley Series in Probability and Statistics, 2003.

[34] N. Piskunov, *Differential and Integral Calculus*, vol. II. Mir Publishers, 1974.

Bhargav Medepally received his Bachelor of Engineering degree in Electronics and Communications Engineering from the Vasavi College of Engineering, Hyderabad, India in 2007. He received his Master of Engineering degree in Telecommunications from the Indian Institute of Science, Bangalore, India in 2009. Since then, he has been with ST-Ericsson, Bangalore, India, working on the physical layer software development for the ST-Ericsson's mobile platforms. His research interests include cooperative communications, energy harvesting networks, and signal processing applications for wireless communications.

Neelesh B. Mehta (S'98-M'01-SM'06) received his Bachelor of Technology degree in Electronics and Communications Engineering from the Indian Institute of Technology (IIT), Madras in 1996, and his M.S. and Ph.D. degrees in Electrical Engineering from the California Institute of Technology, Pasadena, CA, USA in 1997 and 2001, respectively. He is now an Assistant Professor at the Dept. of Electrical Communication Engineering, Indian Institute of Science (IISc), Bangalore, India. Prior to joining IISc, he has held research positions in the Wireless Systems Research group in AT&T Laboratories, Middletown, NJ, USA, Broadcom Corp., Matawan, NJ, USA, and Mitsubishi Electric Research Laboratories, Cambridge, MA, USA.

His research includes work on link adaptation, multiple access protocols, system-level performance analysis of third generation and beyond cellular systems, MIMO and antenna selection, energy harvesting networks, and cooperative communications. He was also actively involved in radio access network physical layer (RAN1) standardization activities in 3GPP. He has served on several TPCs. He was a tutorial co-chair for SPCOM 2010, and was a TPC co-chair for WISARD 2010 and WISARD 2011, the Transmission technologies track of VTC 2009 (Fall), and the Frontiers of Networking and Communications symposium of Chinacom 2008. He is an Editor of the IEEE TRANSACTIONS ON WIRELESS COMMUNICATIONS and an executive committee member of the IEEE Bangalore Section and the Bangalore chapter of the IEEE Signal Processing Society.